

Probing flavor models with ^{76}Ge -based experiments on neutrinoless double- β decay

Matteo Agostini,^{1,2,*} Alexander Merle,^{3,†} and Kai Zuber^{4,‡}

¹*Physik Department and Excellence Cluster Universe, Technische Universität München, Germany*

²*Gran Sasso Science Institute (INFN), L'Aquila, Italy*

³*Max-Planck-Institut für Physik (Werner-Heisenberg-Institut), Germany*

⁴*Institute for Nuclear and Particle Physics, Technische Universität Dresden, Germany*

(Dated: March 5, 2022)

The physics impact of a staged approach for double- β decay experiments based on ^{76}Ge is studied. The scenario considered relies on realistic time schedules envisioned by the GERDA and the MAJORANA collaborations, which are jointly working towards the realization of a future larger scale ^{76}Ge experiment. Intermediate stages of the experiments are conceived to perform quasi background-free measurements, and different data sets can be reliably combined to maximize the physics outcome. The sensitivity for such a global analysis is presented, with focus on how neutrino flavor models can be probed already with preliminary phases of the experiments. The synergy between theory and experiment yields strong benefits for both sides: the model predictions can be used to sensibly plan the experimental stages, and results from intermediate stages can be used to constrain whole groups of theoretical scenarios. This strategy clearly generates added value to the experimental efforts, while at the same time it allows to achieve valuable physics results as early as possible.

Neutrino physics led to big discoveries in the past decades, the greatest being the observation of neutrino oscillations [1], which prove that neutrino masses (albeit tiny) must be non-zero and that neutrino flavors mix. In a nutshell, this means that an electron neutrino does not have a fixed mass but it is rather a quantum-mechanical superposition of several mass eigenstates. While nowadays most oscillation parameters are known [2] and a new era of precision neutrino physics has started, several fundamental questions are still unanswered. Probably the most important question is whether neutrinos have a Majorana nature, i.e., if they are identical to their antiparticles, which would signal a violation of lepton number and thus lead beyond the very successful standard model of particle physics. Such questions can be answered by the observation of neutrinoless double- β decay ($0\nu\beta\beta$) [3], a nuclear transition in which two neutrons decay simultaneously into two protons by emitting two electrons but no neutrino, thus changing lepton number by two units and possibly signaling a Majorana neutrino mass [4].

The experimental search for $0\nu\beta\beta$ is a very active field of particle and nuclear physics. Various isotopes for which $0\nu\beta\beta$ is energetically allowed and many detection techniques are pursued. Examples are: ^{76}Ge with high purity Ge detectors, ^{130}Te with TeO_2 bolometric detectors [5], ^{136}Xe with liquid Xe time projection chambers [6], or Xe-loaded organic liquid scintillator detectors [7]. Historically, ^{76}Ge -based experiments have been leading the field, and the resulting constraints on the half-life of the process are among the most stringent ones [8–10]. Two ^{76}Ge -based experiments are currently active and will yield results in the near future: GERDA [11] and MAJORANA [12]. These two collabo-

rations conceive of eventually realizing a common large scale ^{76}Ge (LSGe) experiment [13], capable of probing the theoretically allowed region for the inverted mass ordering (i.e., the experimentally favorable scenario corresponding to the upper yellow band in FIG. 1). For such a challenging experiment, a highly modular design and a staged approach implementation are needed, meaning that the target mass will be progressively increased.

This paper presents realistic projections of the sensitivity achievable by a global analysis of the data from current and future experiments searching for $0\nu\beta\beta$ in ^{76}Ge . Among $0\nu\beta\beta$ experiments, the ones based on ^{76}Ge stand out because they are designed to perform quasi background-free measurements. Their data can hence be combined without limiting assumptions on the background modeling. We also point out that the sensitivity of a global analysis should be considered when planning the mass-increasing strategy of a project, in order to maximize the benefit for both theory and experiment. Indeed, in case no signal will be observed, large classes of theoretical neutrino models can be excluded already by intermediate stages of an experiment.

The physics observable accessible with $0\nu\beta\beta$ experiments is the *effective Majorana neutrino mass* $|m_{ee}| = |m_1 c_{12}^2 c_{13}^2 + m_2 s_{12}^2 c_{13}^2 e^{i\alpha_{21}} + m_3 s_{13}^2 e^{i(\alpha_{31}-2\delta)}|$, which depends on sines (s) and cosines (c) of the leptonic mixing angles θ_{ij} , the mass eigenvalues, and the phases [14]. It is related to the $0\nu\beta\beta$ half-life by [15]:

$$1/T_{1/2}^{0\nu} = G_{0\nu} |\mathcal{M}_{0\nu}|^2 |m_{ee}|^2, \quad (1)$$

where $G_{0\nu} = 2.42 \cdot 10^{-26} \text{ yr}^{-1} \text{ eV}^{-2}$ is a phase-space factor and $\mathcal{M}_{0\nu}$ is the dimensionless nuclear matrix element (NME) which parametrizes the nuclear physics involved. The allowed range for $|m_{ee}|$ as a function of the smallest neutrino mass m is constrained by the experimental measurements of the neutrino mixing parameters, see FIG. 1. Nevertheless, information about the absolute

* matteo.agostini@ph.tum.de

† amerle@mpp.mpg.de

‡ zuber@physik.tu-dresden.de

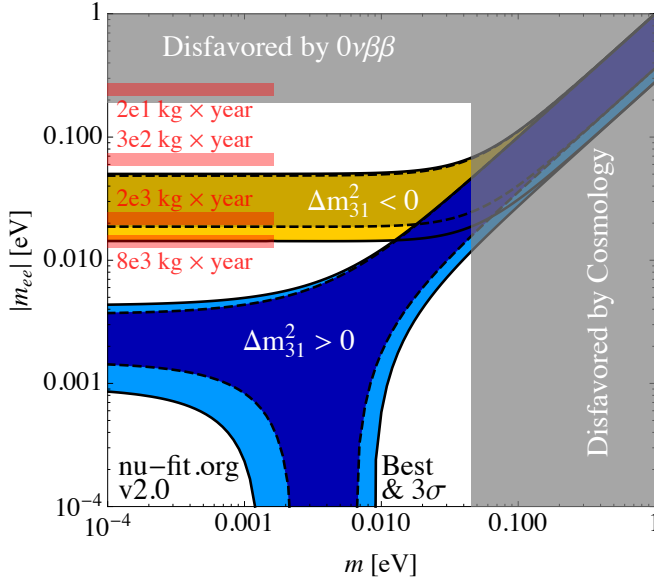


FIG. 1. Most general regions for the effective mass $|m_{ee}|$, calculated using global fit parameters (v2.0) from `nu-fit.org` [2], along with four specific values of sensitivity considered in the text. The broadening of the bands is due to nuclear physics uncertainties. The disfavored regions are the most optimistic bounds from ^{136}Xe -based experiments [6, 7] and Planck [16], the latter converted to the smallest neutrino mass and averaged between both mass orderings.

neutrino mass that is inferred by combining all experimental information are affected by systematic uncertainties of the analysis procedure [17], the NMEs [18], and the mixing parameters [14]. Consequently, even pinning down the neutrino mass ordering – whether normal, $m_1 < m_2 < m_3$ (blue), or inverted, $m_3 < m_1 < m_2$ (yellow) – is challenging.

This situation could drastically change with additional input from neutrino physics. The smallness of neutrino masses can be theoretically explained by suppression mechanisms at tree- [19] or loop-level [20] and the large mixing angles by flavor models based on discrete symmetries [21], which explain them by relating their values to properties of finite symmetry groups. While many of those models yield similar predictions for the accessible observables – so that their experimental distinction is prevented unless the precision is increased by about two orders of magnitude – certain classes of models predict clear *correlations* between observables. Prime examples are *neutrino mass sum rules* [22, 23], such as $\tilde{m}_1 + \tilde{m}_2 = \tilde{m}_3$ or $1/\tilde{m}_1 + 1/\tilde{m}_3 = 2/\tilde{m}_2$, which correlate the complex neutrino mass eigenvalues \tilde{m}_i . These rules are complex equations and thus deliver *two* pieces of information: a constraint on the mass scale m and some relation between the Majorana phases $\alpha_{21,31}$. The most extensive study available [23] investigated more than 50 flavor models divided into 12 classes, which – as FIG. 2 shows – can greatly decrease the allowed range for $|m_{ee}|$, thereby offering the possibilities of gaining valu-

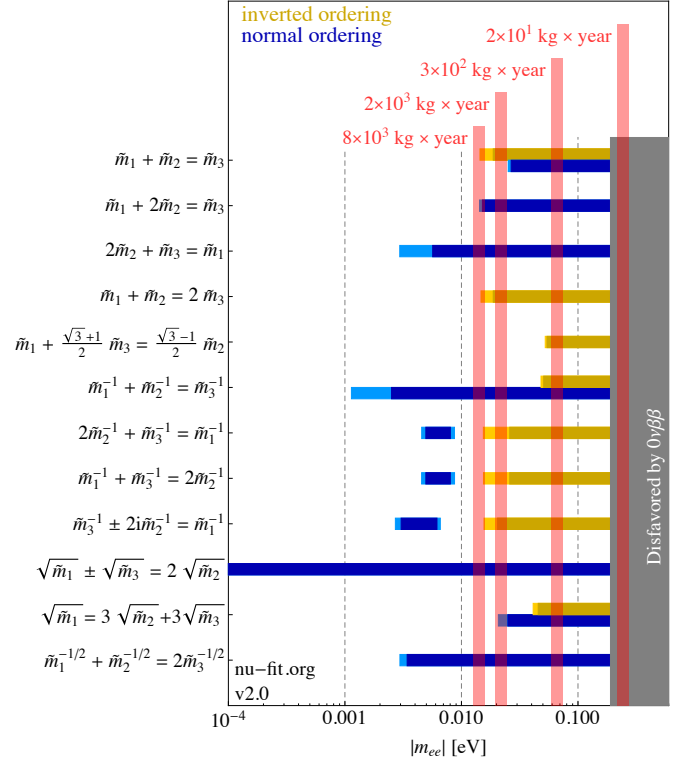


FIG. 2. Range of the $0\nu\beta\beta$ effective mass allowed for different classes of neutrino flavor models that are characterized by respective sum rules. The sensitivity for different stages of ^{76}Ge -based experiments considered in the text is also displayed.

able knowledge on the neutrino sector already by the intermediate steps in a staged approach towards detecting $0\nu\beta\beta$.

The advantages of using high purity Ge (HPGe) detectors for the $0\nu\beta\beta$ search have been recognized early [24]. HPGe detectors can be produced from germanium isotopically enriched in ^{76}Ge ($^{76}\text{Ge}^{\text{enr}}$, typically 87% enrichment). The experimental signature expected for $0\nu\beta\beta$ inside the detector is a peak in the energy spectrum at the Q -value of the ^{76}Ge decay ($Q_{\beta\beta} = 2039.061(7)$ keV [25]). Remarkable advantages of this detection technique are the intrinsic radio-purity of the detectors, the excellent spectroscopic performance ($\lesssim 0.1\%$ energy resolution at $Q_{\beta\beta}$), and the high detection efficiency. In addition, these detectors are a well consolidated technology widely used for γ -ray spectroscopy, which proved to be reliable and suitable for long-term experiments. The detector geometries considered for $0\nu\beta\beta$ experiments include three types: *coaxial*, *Broad Energy Germanium* (BEGe), and *P-type Point Contact* (PPC) [26, 29]. Each geometry results in a specific electric field inside the detector, which affects the performance of event-reconstruction techniques based on the time evolution of the read-out electrical signals (i.e., pulse shape analysis). HPGe detectors must be operated at cryogenic temperatures and are commonly installed in vacuum cryostats. This ap-

proach was adopted also by past $0\nu\beta\beta$ experiments [8, 9], which operated coaxial-type detectors in ultra-low background cryostats surrounded by massive lead and copper shieldings.

Nowadays, the MAJORANA collaboration is pursuing a design based on PPC-type detectors and multiple cryostat modules built from ultrapure electroformed copper. Two modules are currently being assembled (i.e., the MAJORANA DEMONSTRATOR [12]) at the Sanford Underground Research Facility in Lead, South Dakota (USA). The first module hosts 16.8 kg of $^{\text{enr}}\text{Ge}$ detectors and will be fully operational in the second half of 2015. The completion of the second cryostat containing further 12.6 kg of $^{\text{enr}}\text{Ge}$ detectors is scheduled by the end of 2015. The experiment is designed to operate the detectors at a background level of $0.75 \cdot 10^{-3}$ cts/(keV·kg·yr) at $Q_{\beta\beta}$.¹ The GERDA collaboration is instead exploring an alternative design in which an array of bare $^{\text{enr}}\text{Ge}$ detectors is operated directly in ultra radio-pure liquid argon, which acts as coolant material, passive shielding against the external radioactivity, and active veto-system when its scintillation light is detected. The setup is installed in the Gran Sasso underground laboratories of INFN in Italy. GERDA has recently completed its first phase of operation (PHASE I), during which ~ 15 kg of $^{\text{enr}}\text{Ge}$ detectors (mostly of coaxial type) have been operated with a background level of 10^{-2} cts/(keV·kg·yr), yielding a limit of $T_{1/2}^{0\nu} \geq 2.1 \cdot 10^{25}$ yr [10]. The apparatus is currently being upgraded to operate additional 17 kg of $^{\text{enr}}\text{Ge}$ BEGe-type detectors and new sensors for the argon scintillation light. A second data taking phase (PHASE II) is planned to start in the second half of 2015 with a background level of 10^{-3} cts/(keV·kg·yr) at $Q_{\beta\beta}$ [32].

The MAJORANA DEMONSTRATOR and GERDA PHASE II will together start the exploration of $T_{1/2}^{0\nu}$ at the scale of 10^{26} yr, i.e., $|m_{ee}| \sim 0.1$ eV. The results collected by the two experiments during the first years of operation will be essential to define the design of the LSGe experiment and down-select the best technologies to operate $\gtrsim 1000$ kg of target mass at a background level of $\lesssim 10^{-4}$ cts/(keV·kg·yr) at $Q_{\beta\beta}$. With such parameters, the LSGe experiment will probe $T_{1/2}^{0\nu}$ sensitivity at the level of 10^{27} – 10^{28} yr and hence explore an essential part of the parameter space allowed for inverted mass ordering or – with a fortunate value of θ_{12} and better precision on that parameter coming from experiments like JUNO [27] or RENO-50 [28] – even the whole parameter space.

The sensitivity achievable by a global analysis of GERDA PHASE I and PHASE II, the MAJORANA DEMONSTRATOR, and a future LSGe experiment has been studied by assuming the data sets listed in TABLE I. Following the analysis approach adopted by the GERDA collaboration, data from GERDA PHASE I are divided into two

TABLE I. Parameters assumed for each data set: detector mass, efficiency ϵ , background level at $Q_{\beta\beta}$, energy resolution (full width at half maximum, FWHM) at $Q_{\beta\beta}$, start time, and duration of the data taking Δt . The start time of the current (future) experiments is indicated with t_0 (t_1) and expected to be in the second half of 2015 (in the 2020s).

data set	mass [kg]	ϵ	background $\left[\frac{\text{cts}}{\text{keV} \cdot \text{kg} \cdot \text{yr}} \right]$	FWHM [keV]	start time	Δt [yr]
GERDA PHASE I:						
<i>coaxial</i>	12.2	0.62	$1.1 \cdot 10^{-2}$	4.4	Nov 2011	1.3
<i>BEGe</i>	2.8	0.66	$0.5 \cdot 10^{-2}$	2.9	Jul 2012	0.8
GERDA PHASE II:						
<i>coaxial</i>	17.7	0.62	$1 \cdot 10^{-3}$	4.0	t_0	4
<i>BEGe</i>	20.0	0.65	$1 \cdot 10^{-3}$	2.5	t_0	4
MAJORANA DEMONSTRATOR:						
<i>mod1</i>	16.8	0.65	$0.8 \cdot 10^{-3}$	3.0	t_0	4
<i>mod2</i>	12.6	0.65	$0.8 \cdot 10^{-3}$	3.0	$t_0+0.5$ yr	4
Future large scale (LSGe) experiment:						
<i>mod1</i>	200	0.65	$1 \cdot 10^{-4}$	2.5	t_1	10
<i>mod2</i>	200	0.65	$1 \cdot 10^{-4}$	2.5	t_1+1 yr	9
<i>mod3</i>	200	0.65	$1 \cdot 10^{-4}$	2.5	t_1+2 yr	8
<i>mod4</i>	200	0.65	$1 \cdot 10^{-4}$	2.5	t_1+3 yr	7
<i>mod5</i>	200	0.65	$1 \cdot 10^{-4}$	2.5	t_1+4 yr	6

data sets according to the two types of detectors operated.² The separation into two data sets is assumed also for PHASE II. The experimental parameters such as efficiencies, background level and duration are taken from the published values [10, 30]. The energy resolution is taken from the most recent R&D results [30–32]. BEGe-type detectors will provide higher energy resolution and superior background reduction performance with respect to the coaxial type. Data from MAJORANA DEMONSTRATOR are also split between the two modules into two data sets. Efficiencies of PPC- and BEGe-type detectors are assumed to be equal. This assumption is fully consistent with the first results presented by the MAJORANA collaboration [26], and from which the energy resolution is taken. A staged approach is assumed for the LSGe experiments. Given realistic constraints on the production of $^{\text{enr}}\text{Ge}$ material³ the total target mass of 1000 kg is assumed to be progressively increased by installing one new module with 200 kg of detectors per year. The de-

¹ The design goal of the MAJORANA DEMONSTRATOR is typically quoted as 3 cts/(ton·yr) in a region of interest of 4 keV.

² The data set correspond to the “golden” and “BEGe” data sets of Ref. [10]. A third data set considered in the analysis of the collaboration (the “silver” data sets, about 6% of the overall exposure) is not considered here, due to its negligible contribution to the overall sensitivity of the experiment.

³ The Svetlana Department facility can currently deliver 80–100 kg of ^{76}Ge per year [31]. We realistically assume that the production can be doubled in the next years and with some investments coming from the LSGe experiment.

tectors are considered to perform similarly to BEGe-type detectors.

The total number of $0\nu\beta\beta$ events in each data set as a function of $T_{1/2}^{0\nu}$ is given by:

$$N^{0\nu} = \ln 2 \cdot N_A \cdot \epsilon \cdot \eta / (m_a \cdot T_{1/2}^{0\nu}), \quad (2)$$

where N_A is the Avogadro's number, ϵ the efficiency, η the exposure, and m_a the molar mass of ^{76}Ge . In this work, the exposure η is defined as the product of total detector mass and data taking time. The efficiency ϵ is given by the product of four contributions: the fraction of ^{76}Ge in the detectors material ($\sim 87\%$), the fraction of the detector volume which is active (87% for coaxial, 92% for BEGe/PPC detectors), the efficiency of the analysis cuts (90%, dominated by pulse shape analysis cuts), and the probability that $0\nu\beta\beta$ events in the detector active volume are correctly reconstructed at energy $Q_{\beta\beta}$ (92% for coaxial, 90% for BEGe/PPC detectors). These efficiencies are taken from Ref. [10]. A duty cycle of 95% is assumed for all experiments, which accounts for the time needed to calibrate the detectors and for ordinary hardware maintenance.

A statistical approach is adopted to estimate the $T_{1/2}^{0\nu}$ lower limit achievable by a global analysis of the various data sets. More than 10^6 time-stamps are randomly selected. Given a time-stamp, background events with a uniform energy distribution in the range $Q_{\beta\beta} \pm 0.1$ MeV are generated with Monte Carlo techniques. Events are generated independently for each data set according to its background level, exposure, and efficiency. A simultaneous fit of all data sets is hence performed, using a constant probability density function for the background and a Gaussian function for the $0\nu\beta\beta$ signal (with centroid at $Q_{\beta\beta}$). The 90% C.L. upper limit on number of $0\nu\beta\beta$ counts extracted from the fit is converted into a 90% C.L. lower limit on $T_{1/2}^{0\nu}$ by using Eq. (2).

The fit procedure is based on an unbinned profile likelihood analysis in which the number of $0\nu\beta\beta$ counts is bounded to positive values. The free parameters of the fit are the number of signal counts (the parameter of interest) and the background levels (nuisance parameters). Systematic uncertainties (energy scale, resolution, and efficiency) have been studied by adding Gaussian pull terms in the likelihood function and found to worsen the limits by $\lesssim 1\%$. To reduce the computational time, these systematic uncertainties have not been included in the final simulation, as their effect is small for a limit-setting experiment. The coverage of the method has been tested for a sample of time-stamps and found to provide a conservative overcoverage.

The results of these computations are shown in FIG. 3. The top panel illustrates the integrated exposure over time. The increase of exposure is driven by GERDA PHASE I (between 2012 and mid 2013), GERDA PHASE II and the MAJORANA DEMONSTRATOR (between t_0 and t_0+4 yr) and the LSGe experiment (between t_1 and t_1+10 yr). The middle panel shows the

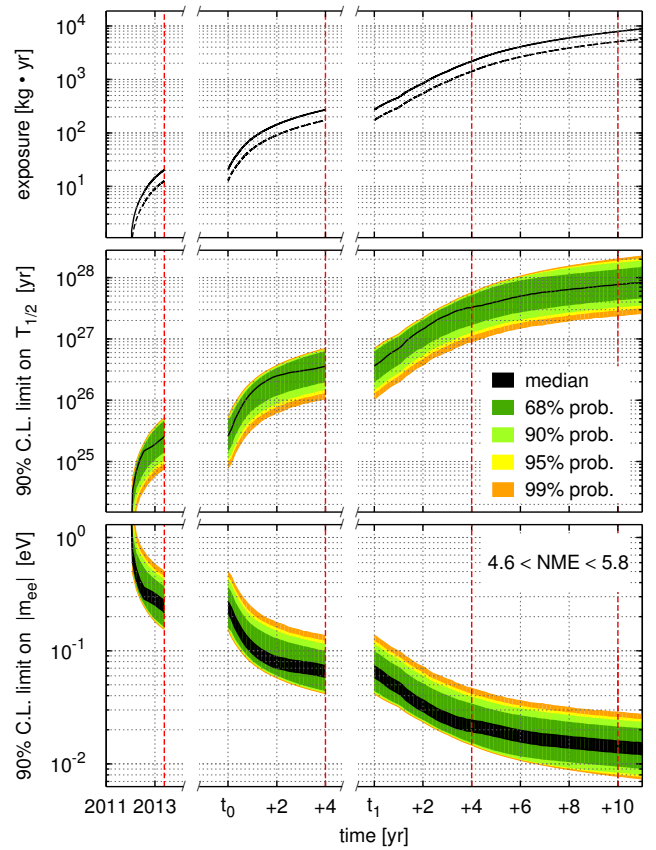


FIG. 3. Top panel: integrated exposure assumed for the calculation as a function of time before (solid line) and after (dashed line) efficiency correction. Middle (bottom) panel: distribution of the 90% C.L. lower limits on $T_{1/2}^{0\nu}$ (upper limits on $|m_{ee}|$) derived by a global analysis of multiple realizations of the experiments. The vertical red lines corresponds to specific values of exposure/sensitivity discussed in the text. The time axis is broken and future dates are given with respect to the start of GERDA PHASE II and the MAJORANA DEMONSTRATOR (t_0), and of the future LSGe experiment (t_1).

distribution of the 90% C.L. lower limits on $T_{1/2}^{0\nu}$. The uppermost part of the distribution is populated by the data set realizations with no background events at $Q_{\beta\beta}$ (i.e., fully background-free). It grows linearly with the exposure and has a sharp cut-off due to the constraint $N^{0\nu} \geq 0$ imposed on the fit. The bottom panel shows the distribution of the 90% upper limits on the effective mass $|m_{ee}|$. This distribution is computed by converting each $T_{1/2}^{0\nu}$ limit through Eq. (1), which introduces an additional systematic uncertainty on each limit due to the uncertain NME calculations. The effect of this systematic uncertainty is maximally included in the plot assuming NME values in the range between 4.6 and 5.8 [23].⁴

⁴ The range covers all the calculations available in the literature except for the shell model, which predicts an outlier value for NME of 2.3 [23]. Expanding the range up to the shell model prediction increases our upper bounds on $|m_{ee}|$ by a factor of 2.

Thus, the median line becomes a band and the central intervals broaden.

FIG. 3 shows how successive experiments can be designed to improve the median experimental sensitivity by an order of magnitude. GERDA PHASE I reached a sensitivity of $T_{1/2}^{0\nu} > 2.6 \cdot 10^{25}$ yr ($|m_{ee}| > 215\text{--}272$ meV) with an exposure of ~ 20 kg·yr (corresponding to the leftmost red line in FIG. 3). GERDA PHASE II and the MAJORANA DEMONSTRATOR will improve the sensitivity up to $T_{1/2}^{0\nu} > 4 \cdot 10^{26}$ yr ($|m_{ee}| > 58\text{--}74$ meV) by collecting an exposure of $3 \cdot 10^2$ kg·yr in 4 yr. The LSGe experiment will finally rise the sensitivity up to $T_{1/2}^{0\nu} > 8 \cdot 10^{27}$ yr ($|m_{ee}| > 13\text{--}16$ meV) in 10 yr of data taking and a final exposure of $8 \cdot 10^3$ kg·yr. It is noteworthy that a sensitivity of $T_{1/2}^{0\nu} > 3 \cdot 10^{27}$ yr ($|m_{ee}| > 19\text{--}24$ meV) can be reached with about $2 \cdot 10^3$ kg·yr in 4 years of data taking with the LSGe experiment.

The ultimate question to answer is what can be learned about neutrino physics from future ^{76}Ge -based experiments. FIG. 1 shows how challenging will be to fully probe the parameter space allowed for $|m_{ee}|$ in the most general situation, even considering the future LSGe and inverted mass ordering. Intermediate sensitivity stages seem not to be able to provide remarkable physics results unless a positive signal is observed. However, we demonstrate in FIG. 2 that whole groups of more specific neutrino flavor models, namely those which predict particular mass sum rules, can be excluded already by intermediate stages. For example, the sum rule $\tilde{m}_1^{-1} + \tilde{m}_2^{-1} = \tilde{m}_3^{-1}$ yields for inverted ordering a smallest allowed neutrino mass of 51 meV (48 meV) for the best-fit (3σ) values of the neutrino mass squares. This region can be almost probed by GERDA PHASE II and the MAJORANA DEMONSTRATOR, and fully probed (i.e., even with *all* uncertainties) by first stages of the LSGe experiment. Thus, by using the sum rule predictions as orientation

when planning the stages, one can exploit the synergies between model predictions and experimental sensitivities to greatly enhance the physics outcome even of the intermediate stages. This synergy goes so far that some groups of models could be distinguished in spite of the uncertainties involved, and our considerations would be strengthened further by a better knowledge on the NMEs, on the neutrino mass ordering, or on the mixing angle θ_{12} – and even more by the observation that the sum rule predictions are quite stable in what regards certain types of theoretical (radiative) corrections [33]. Additionally, we would like to point out that a remarkable number of models could be already ruled out with $\sim 2 \cdot 10^3$ kg·yr of exposure.

Such an exposure could be collected by a single module of the LSGe experiment or by upgrades of GERDA PHASE II and the MAJORANA DEMONSTRATOR which are already under consideration within the experimental community [13, 34].

In conclusion, realistic sensitivity projections have been presented for the current and future ^{76}Ge -based experiments. A global analysis of different data sets is reliable and should be performed. The global sensitivity and its impact on flavor models should be carefully considered when designing the mass-increasing strategy of the future projects.

Synergies between theory and experiment can push us to new frontiers in neutrino physics, provided that we make proper use of them.

ACKNOWLEDGMENTS

M. A. would like to thank A. Caldwell, J. Detwiler, L. Pandola, B. Schwingenheuer, and S. Schönert for valuable discussions. A. M. acknowledges partial support from the European Union FP7 ITN-INVISIBLES (Marie Curie Actions, PITN-GA-2011-289442).

-
- [1] K. A. Olive *et al.* [Particle Data Group Collaboration], Chin. Phys. C **38**, 090001 (2014).
 - [2] M. C. Gonzalez-Garcia, M. Maltoni and T. Schwetz, JHEP **1411** (2014) 052.
 - [3] W. H. Furry, Phys. Rev. **56**, 1184 (1939).
 - [4] J. Schechter and J. W. F. Valle, Phys. Rev. D **25**, 2951 (1982); M. Duerr, M. Lindner and A. Merle, JHEP **1106**, 091 (2011).
 - [5] K. Alfonso *et al.* [CUORE Collaboration], arXiv:1504.02454.
 - [6] J. B. Albert *et al.* [EXO-200 Collaboration], Nature **510** (2014) 229.
 - [7] A. Gando *et al.* [KamLAND-Zen Collaboration], Phys. Rev. Lett. **110** (2013) 6, 062502.
 - [8] M. Günther *et al.*, Phys. Rev. D **55**, 54 (1997).
 - [9] C. E. Aalseth *et al.* [IGEX Collaboration], Phys. Rev. D **65**, 092007 (2002).
 - [10] M. Agostini *et al.* [GERDA Collaboration], Phys. Rev. Lett. **111** (2013) 12, 122503.
 - [11] K. H. Ackermann *et al.* [GERDA Collaboration], Eur. Phys. J. C **73**, no. 3, 2330 (2013).
 - [12] N. Abgrall *et al.* [MAJORANA Collaboration], Adv. High Energy Phys. **2014**, 365432 (2014); W. Xu *et al.* [MAJORANA Collaboration], J. Phys. Conf. Ser. **606** (2015) 1, 012004.
 - [13] Neutrinoless Double Beta Decay Report to the Nuclear Science Advisory Committee (NSAC), April 24, 2014 (<http://science.energy.gov/np/nsac/reports>).
 - [14] M. Lindner, A. Merle and W. Rodejohann, Phys. Rev. D **73**, 053005 (2006); A. Merle and W. Rodejohann, Phys. Rev. D **73**, 073012 (2006).
 - [15] A. Smolnikov and P. Grabmayr, Phys. Rev. C **81**, 028502 (2010).
 - [16] P. A. R. Ade *et al.* [Planck Collaboration], arXiv:1502.01589 [astro-ph.CO].
 - [17] W. Maneschg, A. Merle and W. Rodejohann, Europhys.

- Lett. **85**, 51002 (2009).
- [18] T. R. Rodriguez and G. Martinez-Pinedo, Phys. Rev. Lett. **105**, 252503 (2010); J. Menendez, A. Poves, E. Caurier and F. Nowacki, Nucl. Phys. A **818**, 139 (2009); J. Barea, J. Kotila and F. Iachello, Phys. Rev. C **87**, no. 1, 014315 (2013); J. Suhonen and O. Civitarese, Nucl. Phys. A **847**, 207 (2010); A. Meroni, S. T. Petcov and F. Šimkovic, JHEP **1302**, 025 (2013); F. Šimkovic, V. Rodin, A. Faessler and P. Vogel, Phys. Rev. C **87**, no. 4, 045501 (2013); M. T. Mustonen and J. Engel, Phys. Rev. C **87**, no. 6, 064302 (2013).
 - [19] P. Minkowski, Phys. Lett. B **67**, 421 (1977); T. Yanagida, Conf. Proc. C **7902131**, 95 (1979); M. Gell-Mann, P. Ramond and R. Slansky, Conf. Proc. C **790927**, 315 (1979); S. L. Glashow, NATO Sci. Ser. B **59**, 687 (1980); R. N. Mohapatra and G. Senjanovic, Phys. Rev. Lett. **44**, 912 (1980); M. Magg and C. Wetterich, Phys. Lett. B **94**, 61 (1980); G. Lazarides, Q. Shafi and C. Wetterich, Nucl. Phys. B **181**, 287 (1981); R. Foot, H. Lew, X. G. He and G. C. Joshi, Z. Phys. C **44**, 441 (1989).
 - [20] E. Ma, Phys. Rev. D **73**, 077301 (2006); A. Zee, Phys. Lett. B **161**, 141 (1985); A. Zee, Nucl. Phys. B **264**, 99 (1986); K. S. Babu, Phys. Lett. B **203**, 132 (1988); S. F. King, A. Merle and L. Panizzi, JHEP **1411**, 124 (2014); M. Gustafsson, J. M. No and M. A. Rivera, Phys. Rev. Lett. **110**, no. 21, 211802 (2013) [Erratum-ibid. **112**, no. 25, 259902 (2014)]; M. Gustafsson, J. M. No and M. A. Rivera, Phys. Rev. D **90**, no. 1, 013012 (2014).
 - [21] G. Altarelli and F. Feruglio, Rev. Mod. Phys. **82** (2010) 2701; H. Ishimori, T. Kobayashi, H. Ohki, Y. Shimizu, H. Okada and M. Tanimoto, Prog. Theor. Phys. Suppl. **183** (2010) 1; S. F. King and C. Luhn, Rept. Prog. Phys. **76** (2013) 056201; S. F. King, A. Merle, S. Morisi, Y. Shimizu and M. Tanimoto, New J. Phys. **16** (2014) 045018.
 - [22] F. Bazzocchi, L. Merlo and S. Morisi, Phys. Rev. D **80** (2009) 053003; J. Barry and W. Rodejohann, Nucl. Phys. B **842** (2011) 33; L. Dorame, D. Meloni, S. Morisi, E. Peinado and J. W. F. Valle, Nucl. Phys. B **861** (2012) 259.
 - [23] S. F. King, A. Merle and A. J. Stuart, JHEP **1312** (2013) 005.
 - [24] F. Fiorini, A. Pullia, G. Bertolini, F. Cappellani and G. Restelli, Phys. Lett. B **25** (1967) 602.
 - [25] B. J. Mount, M. Redshaw and E. G. Myers, Phys. Rev. C **81**, 032501 (2010).
 - [26] S. Mertens *et al.* [MAJORANA Collaboration], J. Phys. Conf. Ser. **606**, no. 1, 012005 (2015).
 - [27] M. He [JUNO Collaboration], arXiv:1412.4195 [physics.ins-det].
 - [28] S. B. Kim [RENO Collaboration], arXiv:1412.2199 [hep-ex].
 - [29] M. Agostini *et al.* [GERDA Collaboration], Eur. Phys. J. C **73** (2013) 10, 2583; M. Agostini *et al.*, JINST **6** (2011) P03005.
 - [30] M. Agostini *et al.* [GERDA Collaboration], Eur. Phys. J. C **75**, no. 6, 255 (2015).
 - [31] M. Agostini *et al.* [GERDA Collaboration], Eur. Phys. J. C **75**, no. 2, 39 (2015).
 - [32] B. Majorovits [GERDA Collaboration], Phys. Procedia **61** (2015) 254.
 - [33] J. Gehrlein, A. Merle and M. Spinrath, “RGE Corrections for Neutrino Mass Sum Rules”, *Work in progress*.
 - [34] see material presented at the “LNGS Beyond 2020 Meeting”, 28 Apr 2015, Laboratori Nazionali del Gran Sasso (LNGS), Assergi (L’Aquila), Italy. Web site: <https://agenda.infn.it/conferenceDisplay.py?confId=9608>